Academic Science Journal

Study of Magnetic and Dielectric Properties of Nano-Crystalline Mn-Substituted Zn Ferrites

Roaa R. Ahmed*[1], Tahseen H. Mubarak[1] and Ibrahim H. Mohamed[2]

[1]Department of Physics – College of Science – University of Diyala
[2] Department of Biology – College of Science – University of Diyala

roaaramadan204@yahoo.com

Received: 22 June 2022 **Accepted: 8 October 2022**

DOI: https://doi.org/10.24237/ASJ.01.03.668C

Abstract

In the present work, zinc substituted manganese nano ferrites, $Mn_{1-x}Zn_xFe_2O_4$ ferrites with *x* variable from (0.3,0.7 and 0.9) synthesized by co-precipitation method. To investigate the dielectric characteristics of each sample with relation to frequency. With rising frequency, the loss tangent and the dielectric constant both rapidly decrease before stabilizing at higher frequencies, exhibiting normal ferromagnetic behavior were studied in the frequency range (50Hz -5 MHz). On the basis of XRD, the effect of zinc concentration on Mn_{1-x} Zn_x Fe_2O_4 particle size has been addressed. By using Cu-K radiations in combination with X-ray diffraction, the crystalline phases have been found. The XRD patterns have shown that the specimen has spinal type structure, at room temperature and the particle size decreases with concentrations zinc increasing. Effect of varying concentrations of x on the spontaneous magnetization of distinct Mn_{1-x} Zn_x Fe_2O_4 sample is determined. All of the samples of ferrites were magnetic, either of low or high magnetization, according to our findings. At x=0.9 and x=0.3 respectively. The maximum spontaneous magnetization and the smallest particle size were attained. Hysteresis loops of the materials show exhibit nanocrystals ferromagnetic behavior. The magnetic properties were explained in terms of cation distribution and the effect of grain size.

Keywords: Manganese zinc ferrite $Mn_{1-x}Zn_xFe_2O_4$, magnetic and electric properties

Academic Science Journal

دراسة الخواص المغناطيسية والعازلة للفريتات الزنك البلورية المستبدلة بالمنغنيز

رؤى رمضان احمد، تحسين حسين مبارك و ابراهيم هادي محمد

قسم الفيزياء – كلية العلوم – جامعة ديالى
قسم غلوم الحياة – كلية العلوم – جامعة ديالى

الخلاصة

في هذا البحث تم تحضير منغنيز زنك فرايت النانوي $Mn_{1-x}Zn_xFe_2O_4$ بطريقة الترسيب الكيميائي المشترك مع قيم X متفاوتة (0.3 0.7,0.9,). تم فحص الخصائص العازلة لجميع العينات عند درجة حرارة الغرفة كدالة للتردد. ثابت العزل وظل الخسارة يتناقصان بسرعة مع زيادة التردد ثم يصلان إلى قيمة ثابتة عند الترددات العالية مما يدل على السلوك المغنطيسي الطبيعي الذي تمت دراسته في نطاق التردد (50 هرتز -5 ميجاهرتز). تمت مناقشة تأثير تركيز الزنك على حجم جسيم فريت $Mn_{1-x}Zn_x$ بواسطة حيود الاشعة السينيةXRD . تم تحديد الأطوار البلورية بإشعاعاتCu-Kα . اظهرت أنماط XRD أن العينة لها بنية الاسبنل وفي درجة حرارة الغرفة يتناقص حجم الجسيمات مع زيادة تركيزات الزنك. تم تحديد تأثير تراكيز مختلفة من (Zn^{+2}) على مغنطة تلقائية لعينة $Mn_{1-x}Zn_xFe_2O_4$ المختلفة. لقد توصلنا إلى استنتاج مفاده أن جميع العينات الحديد $Mn_{1-x}Zn_xFe_2O_4$ كانت مغناطيسية إما منخفضة أو عالية المغنطة. تم الحصول على الحد الأقصى للمغنطة التلقائية والحد الأدنى لحجم الجسيمات عند $x = 0.9$ و $x = 0.3$ على التوالي. اظهرت حلقات الهسترة من بلورات منغنيز زنك فرايت $Mn_{1-x}Zn_xFe_2O_4$ المغنطيسي الحديدي في درجة حرارة الغرفة. تم شرح الخواص المغناطيسية من حيث توزيع الكاتيونات وتأثير حجم الحبيبات.

الكلمات المفتاحية: منغنيز زنك فرايت$Mn_{1-x}Zn_xFe_2O_4$, الخواص المغناطسية والكهربائية.

Introduction

Due to their unique magnetic and electrical characteristics, ferrite nanoparticles are significant magnetic materials. Ferrites have excellent electrical characteristics and are used in numerous applications, including microwave and radio frequency [1]. The preparation techniques are crucial since these ferrites' dielectric characteristics are quite sensitive to them. Therefore, selecting a suitable procedure is crucial to obtaining ferrites of excellent quality [2]. Applications in nanomaterials demand the ability to manufacture nanostructures of various shapes and sizes on a wide scale. As a result, significant work has been put into developing the ability to synthesize nanomaterials with specialized magnetic and electrical properties.[3].

In high frequency applications, ferrite materials are advantageous due to their low dielectric behavior. Utilizing low-loss ferrite materials, some dielectric resonator antenna (DRA) characteristics can be actively adjusted [4].

Additionally, the research community is becoming increasingly interested in nano ferrites as they demonstrate a connection between magnetic characteristics and their crystal structure small crystalline size significantly developed the electrical and magnetic properties of ferrites according to reported in literature that, therefore there are many different synthesis techniques such as :co-precipitation [5], Ceramic technique [6], Microwave Combustion method [7], Sol-gel method [8], Solvothermal method [9], the standard solid-state reaction technique [10] and the Polyethyleneglycol-assisted hydrothermal method [11]. The optimum technique for creating nanoparticles was determined to be chemical co-precipitation. The easiest and least expensive process for producing nanoparticles, co-precipitation is one of the best ferrite preparation techniques.

This process yields nanoparticles in massive quantities (powder of grams) in a brief amount of time, together with readily accessible compounds as precursors. Iron salts can be combined with a precipitant like NaOH to create iron oxide nanoparticles [12]. In this method, the nucleation and growth steps interlock, but the particles are usually harvested in the time period before Ostwald ripening fully takes into effect. In the present work polycrystalline samples of manganese zinc ferrite $Mn_{1-x}Zn_xFe_2O_4$ (with x ranging from 0.3, 0.7 and 0.9). Using XRD and FESEM, structural and morphological characteristics of samples were investigated.

Materials and preparation methods

1.1. Media and chemicals

Manganese chloride (II), Zinc (II)chloride and Fe(III) chloride were procured from Merck Company. NaOH were purchased from Sigma Aldrich. From the available commercial sources were purchased the glassware and the deionized water as solvent for solutions preparation.

1. 2. Synthesis of $MnZnFe_2O_4$ ferrite nanoparticles

$MnZnFe_2O_4$ ferrite NPs were synthesized using co-precipitation method. In a typical synthesis experiment $MnCl_2$ (Mw = 125.84gmol^{-1}) and $ZnCl_2$(Mw = 136.286 gmol^{-1}) were dissolved in 50 mL deionized water in two beakers separately. Then $FeCl_3$ (Mw = 162.204 gmol^{-1}) was dissolved in 100 mL. The solutions were poured into beaker and mixed by magnetic stirring for 20 min. 5 g of NaOH dissolved in (100 ml) was added dropwise while continuing stirring. The pH solution must be maintained at 12 during precipitation, and dark grey precipitates were obtained after adding NaOH. To obtain the precipitated particles, the mixture was then heated at 90 °C for 1 hr. The salt residues and other contaminants were subsequently removed from these precipitated particles by repeatedly washing them in deionized water. After that, the powder samples were calcined at 300 °C for 3hr.The powder samples naturally cooled at room temperature after the procedure was complete.

Characterization of $MnZnFe_2O_4$ ferrite nanoparticles

The crystallographic phases of prepared ferrite NPs were studied using X-ray diffraction (Phillips Xpert, Holland) with Cu Kα radiation source (λ = 1.5418 A, 40 mA, and 40 kV) in the 2θ range from 20° to 80°. To investigate the textural properties of prepared ferrite NPs, fourier transform-infrared spectroscopy (FT-IR) has been used a Perkin Elmer FT-IR spectrometer, USA, in the range 300 to 4000 cm^{-1}. The morphology of ferrite NPs samples was studied by field emission scanning-electron microscopy using (FE-SEM, Model Sigma VP,Zeiss, Germany). The magnetic behavior study have been carried out via a Utilizing a vibrating sample magnetometer (VSM) with a (LBKFB model Meghnatis Daghigh Kavir Company) and a maximum applied field of 14.5 kOe. Using an LCR meter (GW Instek LCR-8105G) to measure the dielectric constant (Ɛ'), dielectric loss tangent(tanδ), all samples determined at room temperature.

Academic Science Journal

Results and discussion

2.1. X-ray diffraction

X-ray diffraction (XRD) is done.The X-ray diffraction patterns for all samples of nanoparticles with varying compositions (x = 0.3, 0.7, and 0.9) are displayed in Fig. 1.The peaks were indexed as (111), (220), (311), (220), (311), (222), (400), (422),(511),(400) and (622), the position and relative intensity at all samples were identified perfectly matched with standard JCDPS card no-010-0319, However, for x=0.7 very small peaks are observed indicating non crystalline of manganese nano ferrite Table 1 includes the densities, lattice constants, and crystallite sizes.The Debye-equation Scherer's is used to determine the crystal size. [13].

$$D_{ave} = \frac{0.9\,\lambda}{\beta \cos\theta} \quad \text{..... (1)}$$

where λ is wavelength of radiation used (X-ray), β is the full width of the diffraction line at half maximum and θ the Bragg angle of the of the concerned peak. The formula was used to compute of X-rays density $\rho x\ is$.

$$\rho x = \frac{8M}{Na\text{^}3} \quad \text{..... (2)}$$

where M, N are the molecular weight of the samples, Avogadro number and a is the lattice constant, respectively, where 8 stands for the number of formula units in a unit cell[14].

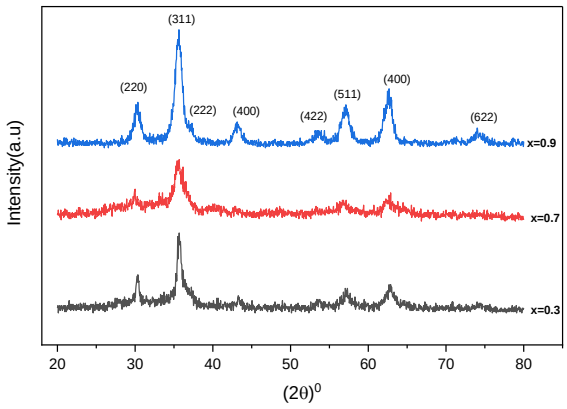

Figure 1: X-Ray diffraction pattern of $MnZnFe_2O_4$ ferrite nano ferrite

Even though all samples were made in the same condition, not all Zn concentrations had the same particle size.

This was most likely caused by the reaction conditions, which encouraged the creation of new nuclei and inhibited particle growth when the Zn concentration was raised without changing the composition, a bigger diameter particle with improved magnetism was created by changing the preparation condition and using the seeding approach.

As a result, controlling the preparation conditions is a useful way to manage particle size the preparation method that used here causes ferrite to develop at varying rates depending on the quantity of Zn, promoting the variety in particle size. [15,16].

Table 1: XRD pattern analysis of $Mn_{1-x}Zn_xFe_2O_4$ ferrite, lattice constant, crystal density and crystalline size.

Molar ratio	sample	Composition	2θ	a(A˚)	dx(gm/cm)	D(nm)
0.3	C1	$Mn_{0.7}Zn_{0.3}Fe_2O_4$	35.712	8.331	9.74	14.7
0.7	C2	$Mn_{0.3}Zn_{0.7}Fe_2O_4$	35.682	8.337	9.72	6.77
0.9	C3	$Mn_{0.1}Zn_{0.9}Fe_2O_4$	35.6	8.354	9.66	7.9

2.2. FT-IR Spectra studies

Fig. (2) shown FT-IR spectra of $Mn_{1-x}Zn_xFe_2O_4$ that had been annealed at 300 ^oC were recorded in the range of 4000-300 cm^{-1}. The 500 cm^{-1} and 400 cm^{-1} characteristic peaks are in good agreement with the Fe-O vibration that serves as the spinel ferrite's distinctive band.

The peaks at 3437.19 cm^{-1} are caused by stretching vibrations of the hydroxyl group (-OH), and the peak at 1635.33 cm^{-1} is caused by -OH bonding of water. These peaks correspond to the essential vibrations and related rotational-vibrational levels, and they reveal the chemical bonds of the prepared particles. The peaks at 460.89 cm^{-1} and 578.64 cm^{-1} imitate the stretching vibrations of Fe-O, Mn-O, and Zn-O that lead to M-O vibrational modes. [17].

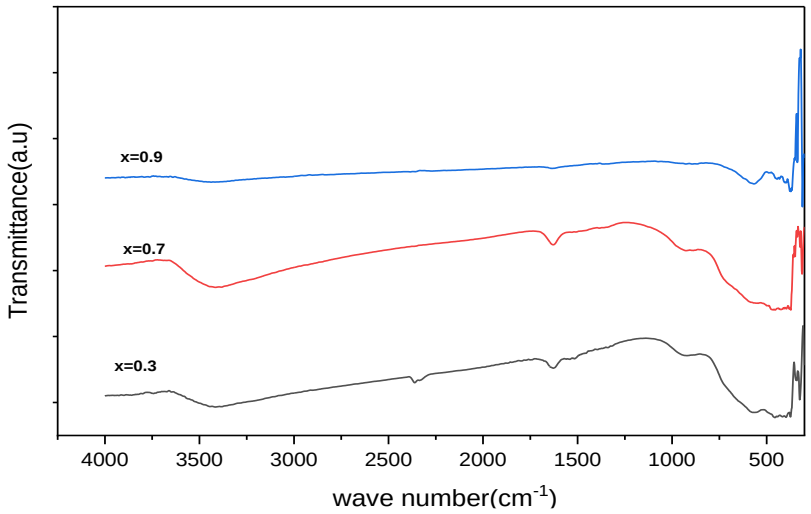

Figure 2: FTIR spectra of $MnZnFe_2O_4$ ferrite nanoparticles

2.3. Morphological (FE-SEM) analysis

Fig. (3). shows the effect of zinc substitution on the morphology of manganese zinc ferrite particles. The average particle size are between 30-60nm, the particle size decreases to a very small extent with increase in the Zn concentration, this may arise when large number of Zn^{2+} ions having small ionic radii (0.74A ˚) replace Mn^{2+} ions having large ionic radii (0.93A ˚) [18]. Field emission scanning electron microscopy analysis (FESEM)analysis revealed at x=0.3 and x=0.9. Agglomerations with a high density imply the presence of poreless crystallites on the surface, because they have high surface energies, the nanoparticles at x=0.7 have a tendency to cluster and develop into larger assemblies.

Academic Science Journal

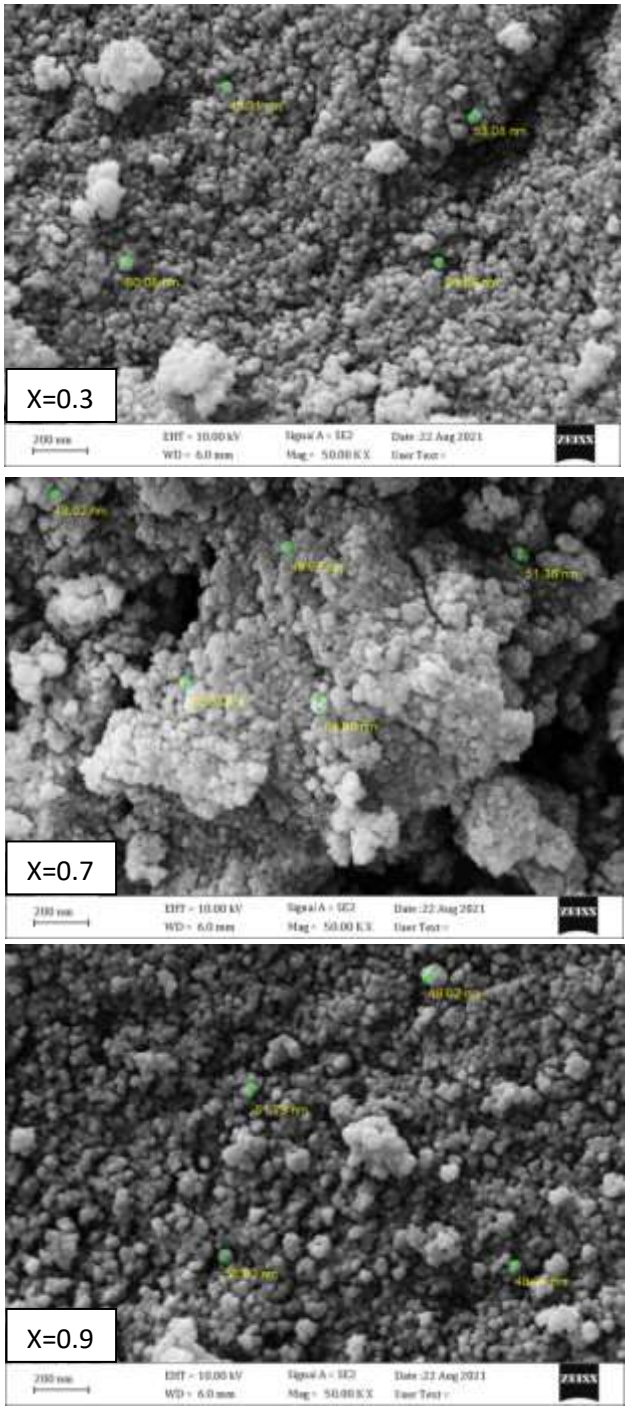

Figure 3: FE-SEM images of $MnZnFe_2O_4$ ferrite nanoparticles

2.4. Magnetic measurements

A vibrating sample magnetometer (VSM) was utilized to examine the magnetic way of behaving of the current ferrite nanoparticles. According to the hysteresis curves that were produced, as illustrated in Fig(4).The relatively small area encircled by the closed curve is connected to the soft magnetic properties of materials.The M-H curve is typical of soft magnetic materials [19]. Were value of saturation magnetization (Ms) in the present study decreases with increasing Zn-substitution from 8.28 (emu/g) to 1.35 (emu/g) when Zn^{2+} ions are replaced with Mn^{2+} ions in the structure. This may be attributed to the inverse spinel structure for $MnZnFe_2O_4$, similar to the manganese spinel ferrite $MnFe_2O_4$, where Zn migrates from A to B sites. Increased Zn^{2+} ion substitution to 0.9 resulted in a higher saturation magnetization of 13.63 (emu/g). anti-ferromagnetic α-Fe_2O_3 phase's presence can be considered to cause a decrease in iron cations distributed on both tetrahedral and octahedral sites as zinc concentrations increase. Thus, it caused an increase in saturation magnetization [20]. Changes in magnetic characteristics were caused by cationic stoichiometry, their occupancy at specific sites, the formation of dead layers on surfaces, the existence of random canting of particle surfaces, non-saturation effects, and variations from the normal cation distribution [21,22]. This is attributed to the variance of cation distribution between tetrahedral and octahedral sites.

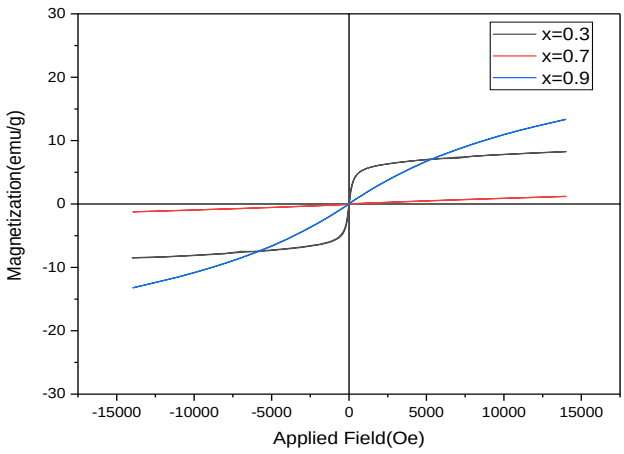

Figure 4: Hysteresis loops of $MnZnFe_2O_4$ ferrite nanoparticle

2.5 Dielectric Properties

The dielectric properties of the $MnZnFe_2O_4$ nanoparticles were analyzed using LCR meter. The dielectric constant were determined from the equations (3) [23].

$$\varepsilon' = \frac{Cd}{\varepsilon_o A} \quad \text{..... (3)}$$

where C is their capacitance, A is the flat surface's cross-sectional area of the pellets in m^2, d is their thickness, and ε_0 is the permittivity of empty space.The behavior of $Mn_{1-x}Zn_xFe_2O_4$ preparation by co-preparation method annelid at 300°C were x=0.3,0.7and 0.9 are shown in Fig.(4).Because electron exchange between Fe^{2+} and Fe^{3+} ions cannot keep up with changes in the externally applied field above a certain frequency, the dielectric constant decreases as frequency increases.[24].

Grain boundaries perform better than grain electrical conduction at lower frequencies, this behavior of a dielectric constant with the substitution of Zn^{+2} ions can be roughly explained by the mechanism of the polarization process in ferrite, which is similar to that in the conduction process.The main cause of the overall polarization in ferrites is the space charge polarization, which is governed by the number of space charge carriers.The density of the localized state and the ensuing displacement of charges with regard to the external field determine the conductivity of the material and the hopping interchange of charges between two localized states. Ionic and orientation sources of polarizability rapidly disappear as the frequency increases duo to the inertia of the molecules and ions. The presence of space charge polarization may be the cause of the present ferrite's high dielectric constant value for x = 0.9 or it could be due to an increase in crystallite size and morphologically clean microstructure[25].This result differs from the researcher[26]. As he noticed the dielectric constant decreases as the values x increase, because increase in zinc concentration leads to an increase grain growth, which is accompanied by a decrease in the grain boundaries, which leads to a decrease in the values of the real dielectric constant, as well as for the imaginary dielectric constant.

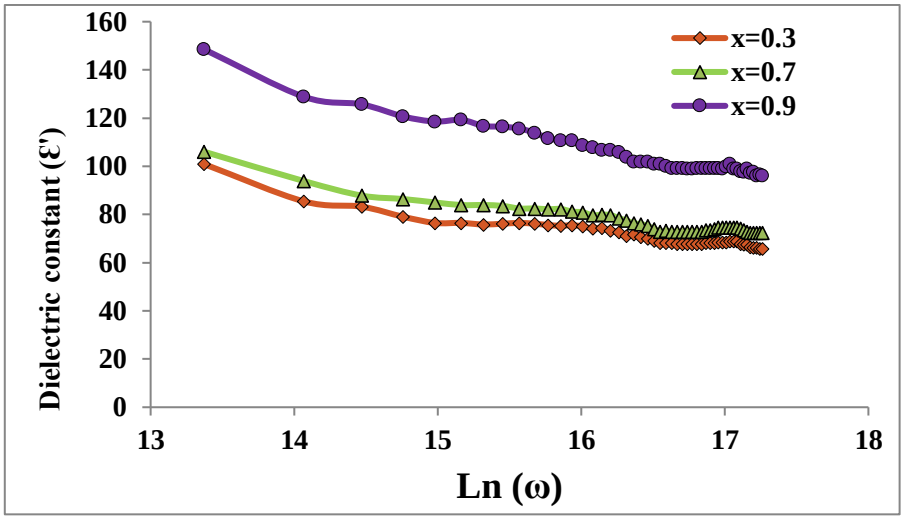

Figure 4: Variation of dielectric constant (ε') as a function of frequency of $Mn_{1-x}Zn_xFe_2O_4$ nanoparticles

2.6 Dielectric Loss

Using the below relation to determine dielectric tangent loss (tanδ) [27]

$$\tan\delta=\frac{\varepsilon''}{\varepsilon'} \quad \text{..... (4)}$$

Where Ɛ′ 'is the real part of the dielectric constant, Ɛ" is the imaginary portion of the dielectric constant, and δ is the loss angle, this represents the amount of energy that the dielectric has absorbed from the alternating field. The dielectric loss serves as a general indicator of the energy dissipation in the dielectric system.

The graph in Fig. 5 illustrates how, at room temperature, the dielectric loss factor varies with frequency.The graph makes it obvious that the dielectric loss falls with frequency and reaches a low value in the high frequency range.According to the study, the dielectric loss abruptly decreased at lower frequencies and stabilized at higher frequencies.Additionally, it was noted that for all samples, the dielectric loss reduced as the frequency increased due to the space charge polarization[28, 29].

Academic Science Journal

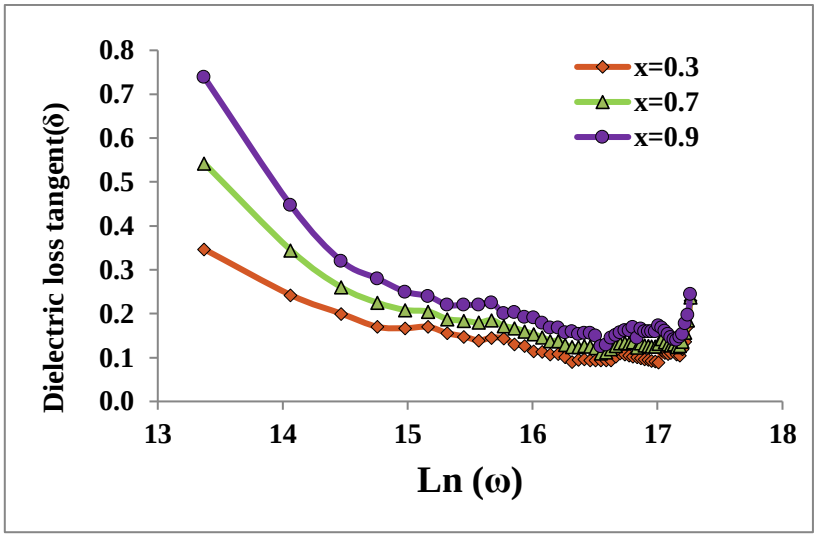

Figure 5: Variation of dielectric loss angle (tanδ)as a function of frequency of $Mn_{1-x}Zn_xFe_2O_4$ nanoparticles (x=0.3,0.7 and 0.9).

Conclusions

The co-precipitation method used to create $Mn_{1-x}Zn_xFe_2O_4$ nanoparticles was explained in this paper. XRD was used to confirm that the $Mn_{1-x}Zn_xFe_2O_4$ nanoparticles belonged to the cubic spinal structure.The $Mn_{1-x}Zn_xFe_2O_4$ nanoparticles' production was also corroborated by the FTIR spectrum.The FE-SEM study also validated and made evident that the nanoparticles aggregated to form spherical-shaped particles. The average crystallite size of MnZn ferrites nanoparticles determined from FESEM were in the range of 30 to 60 nm. For $Mn_{1-x}Zn_xFe_2O_4$ nanoparticles, investigated was how frequency affected on dielectric loss and dielectric constant. Results of dielectric investigations made it clear that frequency had a negative impact on both the dielectric constant and the dielectric loss, which dropped frequency increased.Using VSM measurements, the magnetic characteristics were also investigated.

References

1. J. Chand, K. Gagan, P. Kumar, S. K. Sharma, M. Knobel, M. Singh, J. Alloys and Compds., 509, 9638-9644(2011)

2. K. Gagan, J. Chand, S. Verma, M. Singh, J. Phys. D: Appl. Phys., 42, 155001-155006(2009)
3. M. Gupta, B. S. Randhawa, Solid State Sciences, 14, 849-856(2012)
4. P. B. A. Fechine, R. S. T. Moretzsohn, R. C. S. Costa, J. Derov, J. W. Stewart, A. J. Drehman, C. Junqueira, A. S. B. Sombra, Microwave and Optical Technology Letters**,** 50, 2852–2857(2008)
5. K. M. Batoo, M. S. AbdEl-sadek, J. AlloysCompd., 566,112–119(2013)
6. P. Laokul, V. Amornkitbamrung, S. Seraphin, S. Maensiri, Curr. Appl. Phys.11, 401–408(2011)
7. A. Xia, C. Zuo, L. Chen, C. Jin, Y. Lv, J. Magn. Magn. Mater., 332, 186–191(2013)
8. X. M. Liu, S. Y. Fu, L. P. Zhu, J. Solid State Chem., 180 (2), 461–466(2007)
9. L. J. Zhao, Q. Jiang, J. Magn. Magn. Mater., 322(17), 2485–2487(2010)
10. H. Yang, X. Zhang, W. Ao, G. Qiu, Mater.Res.Bull.,39-833(2004)
11. M. Penchal Reddy, W. Madhuri, G. Balakrishnaiah, N. Ramamanohar Reddy, K. V. SivKumar, V. R. K. Murthy, R. Rama Krishna Reddy, Curr.Appl.Phys.,11,191–198(2011)
12. H. Shokrollahi, Journal of Magnetism and Magnetic Materials, 320(3-4),463-474(2008)
13. M. A. Ahmed, K. E. S. Rady, K. M. El-Shokrofy, A. A. Arais, M. S. Shams, Materials Sciences and Applications, 5, 932-942(2014)
14. A. M. Mohammad, S. M. Ali Ridha, T. H. Mubarak, International Journal Of Applied Engineering Research, 13(8), 6026-6035(2018)
15. B. Jeyadevan, C. N. Chinnasamy, K. Shinoda, K. Tohji, J. Appl. Phys., 93 (10), 8450(2003)
16. K. Parekh, R. V. Upadhyay, R. V. Mehta, J. Appl. Phys., 88 (5), 2799(2000)
17. P. Thakur, D. Chahar, S. Taneja, N. Bhalla, A. Thakur, Ceramics international, 46(10), 15740-15763(2020)
18. R. Arulmurugan, B. Jeyadevan, G. Vaidyanathan, S. Sendhilnathan, Journal of Magnetism and Magnetic Materials, 288, 470-477(2005)

19. Y. Q. Wang, R. M. Cheng, Z. Wen, L. J. Zhao, European Journal of Inorganic Chemistry, 42–47(2011)

20. J. M. Byrne, V. S. Coker, E. Cespedes, P. L. Wincott, D. J. Vaughan, R. A. D. Pattrick, G. van der Laan, E. Arenholz, F. Tuna, M. Bencsik , J. R. Lloyd, N. D. Telling, Advanced Functional Materials, 24(17), 2518–2529(2014)

21. P. Hu, H. B. Yang, D. A. Pan, H. Wang, J. J. Tian, S. G. Zhang, J. Magn. Magn. Mater., 322, 173(2010)

22. L. Nalbandian, A. Delimitis, V. T. Zaspalis, E. A. Deliyanni, D. N. Bakoyannakis, E. N. Peleka, Microporous Mesoporous Mater., 114, 465 (2008)

23. F. G. Brockman, P. H. Dowling, W. G. Steneck, Phys. Rev.,75, 1440(1949)

24. G. R. Mohan, D. Ravinder, A.V. Ramana Reddy, B. S. Boyanov, Materials Letters, 40, 39-45(1999)

25. D. El Kony, Egyptcian Journal of Solids, 27, 285-297(2004)

26. J. Iqbal, M. Rajpoot, T. Jan, I. Ahmad, Journal of Superconductivity and Novel Magnetism, 27(7), 1743-1749(2014)

27. A. Maqsood, K. Khan, J. Alloys Compd., 509, 3393-3397(2011)

28. S. Sagadevan, International journal of Physical Sciences, 8(21),1121-1127(2013)

29. S. Sagadevan, Journal of Nano Research, 34,91-97(2015)